Exploring phase transitions of the 2D Ising model using Markov Chain Monte Carlo method

Sigurd S. Vargdal, Brage A. Trefjord, Nils E. C. Taugbøl and Frida O. Sørensen*
University of Oslo, Department of Physics
(Dated: January 13, 2023)

We seek to apply numerical methods to the two-dimensional Ising model. We compare our results to the already found analytical results. We want to find an approximation to the critical temperature T_c of an infinite two-dimensional Ising model. We apply the Markov chain Monte Carlo method to Ising models of a two-state paramagnet with varying temperatures and lattice sizes, and compute the average energy magnetization. We get an approximated critical temperature with a relative error of 0.05% even with multiple computational difficulties.

Keywords: Ising model, Markov chain Monte Carlo, critical temperature

I. INTRODUCTION

The Ising model is a simple model of particularly connected nodes which contain a specific value, in most cases binary values. The core of the model is that the value of a given node can alternate over time depending on the value in its neighbouring nodes. Originally this model was created to study phase transitions in a one-dimensional ferromagnet by Ernest Ising in 1924 [1]. Ising correctly proved that no phase transition can happen in one dimension but wrongly concluded that his result generalises to higher dimensions [2]. For higher dimensions, the Ising model has proved highly applicable for the study of phase transitions and to this day it has found use in numerous fields [3, 4]. Although the one-dimensional Ising model was analytically solved soon after its creation, the two-dimensional model was not solved analytically until 1944 by Lars Onsager [5].

The behaviour of the Ising model for different systems is of interest and its applicability moves beyond two dimensions. Numerical approaches are then necessary to simulate the Ising model and extrapolate the behaviour and characteristics of the system in question. In this report we will apply a Markov chain Monte Carlo method to a two-dimensional Ising model to find the critical temperatures of two-state paramagnets of finite periodic lattice sizes at fixed temperatures. The results for the finite models will be used to find an approximation to the critical temperature of a model of infinite size.

The report is structured as follows. In Section II we introduce the necessary background for the Ising model and present an overview of Markov chain Monte Carlo methods. In Section III we present the results obtained through various simulations of the Ising model. We also present analytical results as a benchmark for our simulations and consider possible future work. Then, in Section IV we go into a detailed discussion of our results and contemplate how reliable our approach is. We also consider possible improvements. Finally, in Section V we conclude by summarising our discussion.

II. METHOD

A. The Ising model

We will be looking at a two-dimensional Ising model consisting of two-state spins and periodic boundaries. The model will be a two-dimensional grid containing a total number of spins N which in turn is defined by the lattice size L

$$N = L^2. \tag{1}$$

The model grid will always be square in our case and so we will in this report refer to the grid by its lattice size L, we will explore multiple lattice sizes. Each entry in the lattice contains a spin value $s_{i,j}$ which can take two possible values ± 1. We can now represent the model as a matrix

$$\mathbf{s} = \begin{bmatrix} s_{L,1} & \cdots & s_{L,L} \\ \vdots & \ddots & \vdots \\ s_{1,1} & \cdots & s_{1,L} \end{bmatrix}. \tag{2}$$

Every possible configuration of $\mathbf{s}$ is a *microstate*. We will implement periodic boundary conditions by taking the modulo of the indices i and j

$$s_{i,j} = s_{i \bmod L, j \bmod L}. \tag{3}$$

This will wrap each end of the finite rows and columns of the model to their respective starts. For a lattice of size $L = 2$ we will have

$$s_{i,j} = s_{i+2,j} = s_{i,j+2} = s_{i-2,j} = s_{i,j-2}, \tag{4}$$

* Repository:
https://github.com/NilsECT/FYS3150/tree/main/Project_4/

where we can see that the grid repeats itself, and so simulates periodic boundaries.

The Ising model represents in our case a two-state paramagnet where each spin will have its spin-value and energy defined by its immediate neighbours. The energy $E(\mathbf{s})$ of the system for a given microstate $\mathbf{s}$ will be given as the sum of all components $s_{i,j}$ in the grid multiplied with its neighbour and a coupling constant J. We do not count the diagonal neighbours. We express the macroscopic (total) energy of the system through

$$E(\mathbf{s}) = -J \sum_{\langle kl \rangle} s_k s_l, \tag{5}$$

where k and l are neighbouring pairs of spins and we do not double count the spin pairs. This is done by calculating, for every spin, only the right and upper neighbours. This means that for a spin $s_{i,j}$ its contribution to the energy will be decided by $s_{i,j+1}$ and $s_{i+1,j}$. The sum is then expressed as

$$E(\mathbf{s}) = -J \sum_{i,j=1}^{L} (s_{i,j}s_{i,j+1} + s_{i,j}s_{i+1,j}). \tag{6}$$

The total magnetization $M(\mathbf{s})$, for a given microstate $\mathbf{s}$, is decided by the sum of all spins in the lattice

$$M(\mathbf{s}) = \sum_{i,j=1}^{L} s_{i,j}. \tag{7}$$

We can apply this to a lattice $L = 2$. This model will have four spins which each can take one out of two possible values, so there are $2^4 = 16$ microstates for the system. We discriminate each microstate by the number of positive spins that they contain. This means that there will be multiple possible microstates for a given macrostate, the number of microstates that describe the same macrostate is the *degeneracy* of the macrostate. The possible macrostates for this $L = 2$ case can be found in Table I. The derivation of these values can be found in Appendix A.

Table I: The possible total energies and magnetizations for a $L = 2$ model and their degeneracy.

Number of spin up	Degeneracy	Energy	Magnetization
0	1	$-8J$	-4
1	4	0	-2
2	4	0	0
2	2	$8J$	0
3	4	0	2
4	1	$-8J$	4

In the case of the two-state paramagnet, the probability for the lattice to be in a given microstate $\mathbf{s}$ with a total energy $E(\mathbf{s})$ is given by the Boltzmann distribution [6, 220–251]

$$p(\mathbf{s}, T) = \frac{1}{Z} e^{-\beta E(\mathbf{s})}, \tag{8}$$

where $\beta = 1/(k_B T)$ where k_B is the Boltzmann constant and T is the temperature of the model. The partition function Z is a sum of all the Boltzmann factors

$$Z = \sum_{\mathbf{s}} e^{-\beta E(\mathbf{s})}, \tag{9}$$

and acts as a normalisation factor for the distribution.

With the probability distribution we can compute the expectation values of a model at a fixed temperature T. This is desirable to compute other characteristics of the model at given temperatures. The expectation value (average) of the energy is given by the sum over all microstates' energy factorised with their respective probability

$$\langle E \rangle = \frac{1}{Z} \sum_{\mathbf{s}} E(\mathbf{s}) e^{-\beta E(\mathbf{s})}. \tag{10}$$

Similarly we find the expectation value of the energy squared

$$\langle E^2 \rangle = \frac{1}{Z} \sum_{\mathbf{s}} E(\mathbf{s})^2 e^{-\beta E(\mathbf{s})}. \tag{11}$$

The expectation values for the absolute total magnetization and its square are found similarly

$$\langle |M| \rangle = \frac{1}{Z} \sum_{\mathbf{s}} |M(\mathbf{s})| e^{-\beta E(\mathbf{s})}, \tag{12}$$

and

$$\langle M^2 \rangle = \frac{1}{Z} \sum_{\mathbf{s}} M(\mathbf{s})^2 e^{-\beta E(\mathbf{s})}. \tag{13}$$

The two properties which will be of interest to us are the *specific heat capacity* C_V and the *magnetic susceptibility* χ. The specific heat capacity is the amount of heat absorbed by a system to raise its temperature by one degree. The specificity is descided by the size of the model, i.e. the total number of spins. The magnetic susceptibility is a proportionality constant that relates how the magnetic configuration of a system reacts to an external magnetic field. The specific heat capacity is given by

$$C_V = \frac{1}{N} \frac{1}{k_B T^2} (\langle E^2 \rangle - \langle E \rangle^2), \tag{14}$$

where we normalise to the total number of spins. The magnetic susceptibility is given by

$$\chi = \frac{1}{N} \frac{1}{k_B T} (\langle M^2 \rangle - \langle |M| \rangle^2), \tag{15}$$

which is also normalised to the total number of spins.

We note that the magnetization and energy can be divided by the total number of spins N to give the energy per spin ϵ and the absolute magnetization per spin $|m|$. Their expectation values are computed completely analog to E and M.

The spins in the model have a probability of changing their value depending on the difference in energy they have to their neighbours. This is the core idea of the Ising model. A chosen spin (or entry) has a probability of changing its value decided by the configuration of its immediate neighbours at a given time step. We call a change in value for a spin a *flip*. We will simulate the evolution of the Ising model using the Markov chain Monte Carlo method, which is introduced bellow. This simulaton requires the Boltzmann factor of the difference in energy of the system when a single spin is flipped

$$e^{-\beta \Delta E}. \tag{16}$$

Here, ΔE is the energy difference we get from flipping one spin. We note that ΔE can only take five possible values since every spin has only four neighbouring spins which will contribute differently to the total energy. The possible values of ΔE are only dependent on how many of the neighbouring spins have a value $+1$ (since the other spins then must be -1). This trait allows us to compute the five possible values $e^{-\beta \Delta E}$ can have when a single spin is flipped before simulating the evolution of the model.

In the exemplary case of a model with lattice $L = 2$, we can find analytical expressions for the partition function Z, and the expectation values $\langle \epsilon \rangle$, $\langle \epsilon^2 \rangle$, $\langle |m| \rangle$ and $\langle m^2 \rangle$. These can in turn be used to find expressions for the specific heat capacity C_V and the magnetic susceptibility χ. For the full derivation of these see Appendix B. Here we will simply state the resulting expressions. The partition function for $L = 2$ is

$$Z = 2\left(6 + e^{8\beta J} + e^{-8\beta J}\right).$$

The expectation value of ϵ is

$$\langle \epsilon \rangle = \frac{4J}{Z}(e^{-8\beta J} - e^{8\beta J}),$$

and the expectation value of ϵ^2 is

$$\langle \epsilon^2 \rangle = \frac{8J^2}{Z}\left(e^{8\beta J} + e^{-8\beta J}\right).$$

The expectation value of the absolute value of the magnetization $|m|$ is

$$\langle |m| \rangle = \frac{4 + 2e^{8\beta J}}{Z},$$

and the expectation value of the magnetization squared m^2 is

$$\langle m^2 \rangle = \frac{2}{Z}\left(1 + e^{8\beta J}\right).$$

The specific heat capacity C_V is

$$C_V = \frac{128}{k_B T^2}\frac{J^2(3Z - 16)}{Z^2},$$

and the magnetic susceptibility χ is

$$\chi = \frac{16}{Z^2 k_B T}(3 + 3e^{8\beta J} + e^{-8\beta J}).$$

From our model we want to compute the critical temperature T_c. This is the temperature where the system undergoes a phase transition from a magnetized phase to a phase with no net magnetization. If the model has more spins up $(+1)$ than spins down (-1), it has a positive net magnetization. If it is other way around the net magnetization is negative. The phase transition happens when there is approximately an equal number of spins up as spins down. At the critical temperature, the magnetic susceptibility χ of the model reaches a peak, since the magnetization will not be defined in a specific direction. The paramagnet will not be well aligned with an external magnetic field.

During a phase transition, at the critical temperature, the temperature change should be minimal as energy is used to change the configuration of the model rather than increasing the temperature. The specific heat capacity reaches a maximum at the critical temperature as well.

We expect our model to become more realistic as the lattice size L increases. Specifically, we want to find the critical temperature as L approaches infinity. The critical temperature scales as

$$T_c(L) = aL^{-1} + T_c(L = \infty), \tag{17}$$

where a is a constant. We can therefore compute T_c for different values of L^{-1}, using either χ or C_V as stated above, for which we can perform a first-order linear fit to $T_c(L)$. As we can see in equation 17, the intercept of the fit will be an approximation to $T_c(L = \infty)$. Lars Onsager found the critical temperature at $L = \infty$ for the two-dimensional Ising model [5] to be

$$T_{c,analytical}(L = \infty) = \frac{2}{\ln\left(1 + \sqrt{2}\right)} J/k_B \approx 2.269 J/k_B,$$

which we will use to compare with our numerical result.

B. Markov chain Monte Carlo

The Ising model evolves based on the probability of a randomly chosen spin to flip. The evolution of the model requires that a new randomly chosen spin is given a chance to flip at each iteration. The Markov chain Monte Carlo method (MCMC) is a particularly well suited method to simulate the evolution of Ising models. The general idea is as follows. We start at an arbitrary state $\mathbf{s}_{i=0}$, and suggest a new state $\mathbf{s}_{\text{proposal}}$ on a probability distribution that only depends on $\mathbf{s}_i$. We then apply an *acceptance rule* so that the new state is accepted only if some condition is satisfied. If a proposed new state is accepted the model evolves to the proposed new state. If the proposed new state is rejected, it is discarded and we generate a new proposal, and repeat the procedure. In this report, the acceptance rule will be to generate a random number $r \in [0, 1]$, and apply the acceptance condition

$$r < \min(1, p(\mathbf{s}_{\text{proposal}})/p(\mathbf{s}_i)). \tag{18}$$

Here we see that if the proposal is more probable than the current state, then the ratio will be smaller than one. This means that the model will evolve toward the most probable state, i.e. the *equilibrium point*. We can note that if the current state is among the most probable ones, the iterations will oscillate around the equilibrium point. The probability of each state can be computed through equation 8. Since both microstates $\mathbf{s}_i$ and $\mathbf{s}_{\text{proposal}}$ have the same partition function Z, the acceptance rule will be as follows

$$r < \min(1, e^{-\beta \Delta E}).$$

The full derivation can be found in Appendix C. Every new proposal is an iteration and so

$$\mathbf{s}_{i+1} = \begin{cases} \mathbf{s}_{\text{proposal}}, & \text{if accepted} \\ \mathbf{s}_i, & \text{if rejected} \end{cases}. \tag{19}$$

For the Ising model the suggested state $\mathbf{s}_{\text{proposal}}$ is the state $\mathbf{s}_i$ where a random spin has been flipped. For every iteration we compute the energy E_i and magnetization M_i of the model. These iterations make up the Markov chain, also known as a random walk where every new state is completely dependent on the previous one. We perform the Markov chain sampling for a chosen number of iterations, in this report N iterations, which constitutes one Monte Carlo cycle. We perform a chosen number of cycles to let the model evolve towards its equilibrium point. Each cycle starts where the previous stopped and so the model evolves somewhat continuously. We can then produce approximations to the desired expectation values by summing all energy and magnetization samples and dividing by the total number of Monte Carlo cycles. The approximated expectation value of the energy will then be

$$\langle \tilde{E} \rangle = \frac{1}{N_C} \sum_i E_i, \tag{20}$$

where N_C is the total number of cycles and the approximation is denoted by the tilde. As the system will evolve to its equilibrium point, a large enough amount of cycles will weight $\langle \tilde{E} \rangle$ toward $\langle E \rangle$. An outline of the MCMC method applied on the Ising model can be see in Algorithm 1.

Algorithm 1: Markov chain Monte Carlo

```
s_0 ← [s_{1,1}, s_{1,2}, ..., s_{N,N}] ▷ Generate an initial state
for Number of cycles do
    for N number of spinflips do
        s_proposal ▷ Generate a proposal state by flipping one spin
        r ∈ U(0,1) ▷ Random number between 0 and 1
        if r < min(1, P(s_proposal)/P(s_i)) then
            s_{i+1} = s_proposal ▷ Keep new state
        end
        else
            s_{i+1} = s_i ▷ Keep last state
        end
        Calculate E and |M| for the grid.
    end
    Compute the average of ϵ and |m|.
end
Compute ⟨Ẽ⟩ and ⟨|M̃|⟩.
```

The MCMC has two weaknesses that must be addressed. Firstly, the initial state $\mathbf{s}_0$ might be far away from the equilibrium point. In that case, the model will need a first set of cycles to evolve closer to the equilibrium point. This first set of cycles can shift $\langle \tilde{E} \rangle$ and other approximated expectation values in an undesirable way and so we discard that first set of cycles. This is known as the *burn-in time*. The burn-in time should be tuned to best fit the model in question. Too small a burn-in time will shift the computed mean. Too large a burn-in time will unnecessarily extend the amount of computations. Second, the Monte Carlo cycles are not independent and identically distributed (iid). This means that the approximated expectation values are sensitive to the amount of cycles (and burn-in time if implemented). This can be solved by averaging over MCMC applied to iid initial states, which would provide us with a confidence interval.

III. RESULTS

For a lattice size of $L = 2$, we compared the averages obtained from several Monte Carlo cycles to the ana-

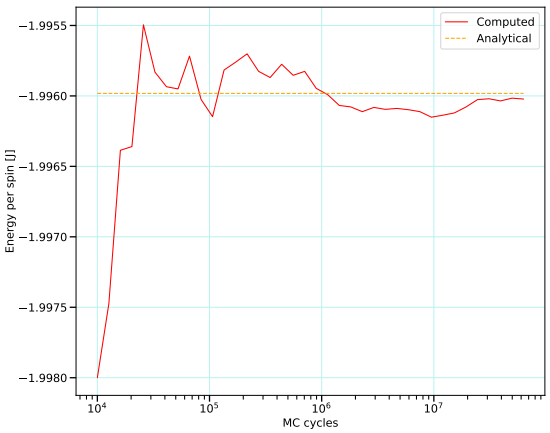

Figure 1: Convergence of $\langle\epsilon\rangle$ to the analytical result of energy per spin as the number of Monte Carlo cycles increases. The value of $\langle\epsilon\rangle$ was computed for a grid of dimensions 2×2, for a temperature of $T = 1J/k_B$.

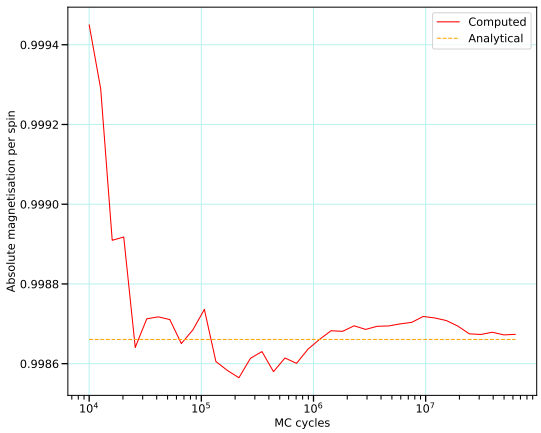

Figure 2: Convergence of $\langle|m|\rangle$ to the analytical result of absolute magnetization per spin as the number of Monte Carlo cycles increases. The value of $\langle|m|\rangle$ was computed for a grid of dimensions 2×2, for a temperature of $T = 1J/k_B$.

lytically calculated values that can be derived from the theory. Every Monte Carlo cycle contributes to each of the total averages with a single averaged value. This was done for a grid of temperature $T = 1J/k_B$. The values we chose to compare are the average energy per spin $\langle\epsilon\rangle$, the average absolute magnetization per spin $\langle|m|\rangle$, the specific heat capacity C_V, and the magnetic susceptibility χ. Each of the computed values are plotted as a function of the number of cycles in Figures 1, 2, 3, and 4 respectively.

Once the MCMC simulation of the $L = 2$ model gave acceptable results, we sampled the distribution of the energy per spin, ϵ, for different temperatures. The sampling was done from 2000 Monte Carlo cycles each. To get an unbiased distribution we sampled from 25 different initial random microstates. The resulting distributions are shown in Figures 5, 6, 7 and 8, where we have also applied a kernel density estimation to the distribution. To get a better understanding of the evolution of the distribution of ϵ we sampled its distribution for four temperatures in the interval $T = [1, 2.4]J/k_B$.

The next step was to look at the convergence of $\langle\epsilon\rangle$ and $\langle|m|\rangle$ as a function of Monte Carlo cycles in order to find a fitting burn-in time and total number cycles. We computed the expectation values with increasing Monte Carlo cycles for both ordered (all spins are +1) and unordered (random) initial states for a range of different temperatures with $L = 20$. We computed the expectation values from 25 up to 10^4 cycles with a step size of 25 cycles. This can be seen in Figure 9 for $\langle\epsilon\rangle$ and in Figure 10 for $\langle|m|\rangle$. Again, we sampled over 25 independent simulations for both ordered and unordered initial

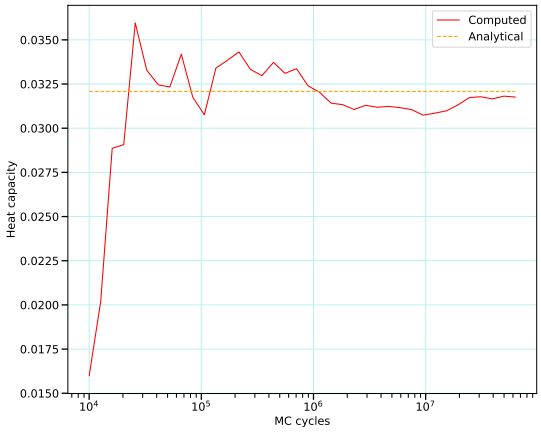

Figure 3: Convergence of C_V to the analytical result of the specific heat capacity C_V as the number of Monte Carlo cycles increases. The specific heat capacity was computed for a 2×2 grid, with temperature $T = 1J/k_B$.

states which allowed us to compute a 95% confidence interval. We note that the ordered initial states' evolution were independent from the other samples. Our burn-in time was chosen and applied based on the convergence in Figures 9 and 10 for the simulations that followed.

We preformed a detailed scan between the temperatures of $T = 2.1$ and $T = 2.6$, with highest reso-

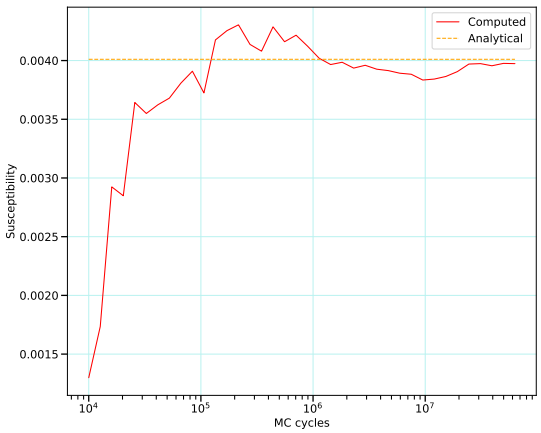

Figure 4: Convergence of χ to the analytical result of the magnetic susceptibility χ as the number of Monte Carlo cycles increases. The magnetic susceptibility was computed for a 2×2 grid, with temperature $T = 1J/k_B$.

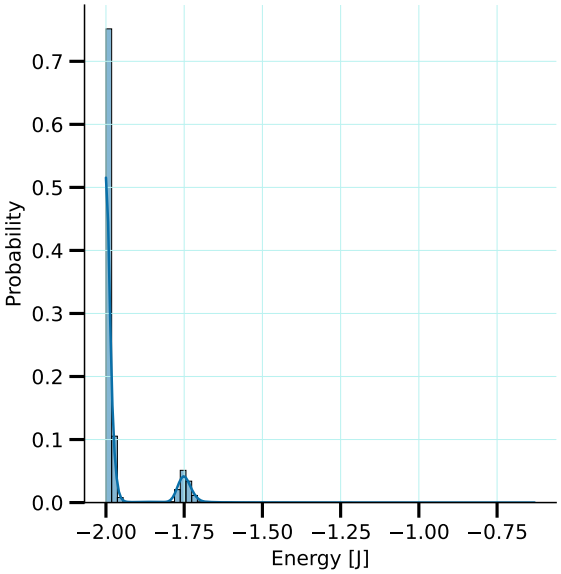

Figure 5: The probability distribution of ϵ at temperature $T = 1J/k_B$ generated from 25 independent simulations using the MCMC method with 2000 cycles.

lution in the are where we expected the critical temperature to be $[2.25, 2.35]$. We did so for lattice sizes $L = 20, 40, 60, 80, 100$ and a single sample. In Figure 11 we see how the temperature affects the specific heat capacity of the different lattice sizes. In Figures 12, 13

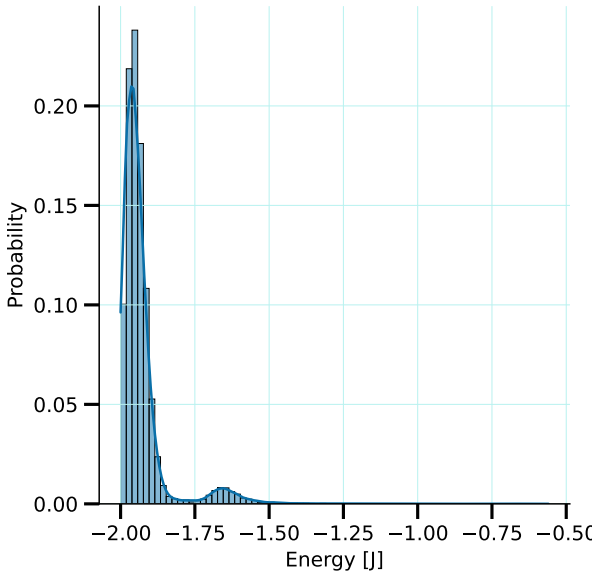

Figure 6: The probability distribution of ϵ at temperature $T = 1.5J/k_B$ generated from 25 independent simulations using the MCMC method with 2000 cycles.

Table II: Numerical approximation and analytical value of the critical temperature as $L \to \infty$. The analytical value we compare with is the value computed by Lars Onsager in 1944. We have also included the relative error.

	$T_c(L = \infty)$	Relative error
Numerical	$2.270 \pm 0.003 J/k_B$	0.05%
Analytical	$2.269 J/k_B$	

and 14 we see how χ, $\langle \epsilon \rangle$ and $\langle |m| \rangle$, respectfully, vary depending on the temperature of their respective lattices.

We find the different critical temperatures T_C of the paramagnet the magnetic susceptibility. Our reasoning was that χ's peaks are the most distinct comparing to the peaks from the specific heat capacity, as can be seen for the axis values in Figures 11 and 12. We extract the temperature of the of the five highest values of χ for each simulated model. We computed the average of these five temperatures which we used as an approximation to T_C for the given model. A first order linear regression was then performed on these approximations as a function of their lattice size. This regression can be seen in Figure 15. Our final approximation to T_C when $L \to \infty$ was then extrapolated as the intercept of the aforementioned linear fit. Our result along with the analytical result can be seen in Table II.

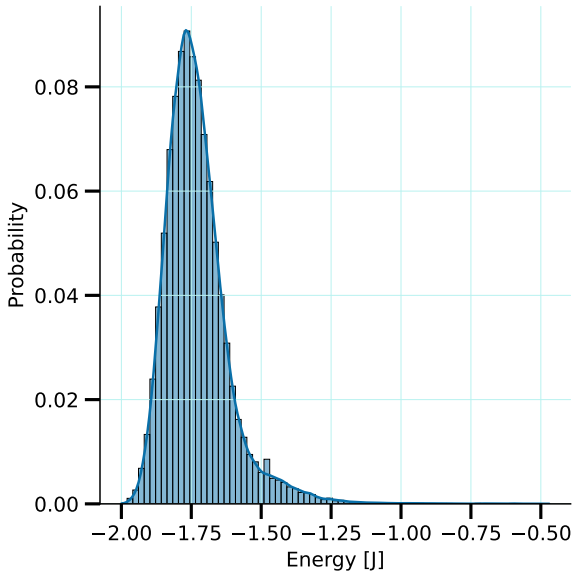

Figure 7: The probability distribution of ϵ at temperature $T = 2J/k_B$ generated from 25 independent simulations using the MCMC method with 2000 cycles.

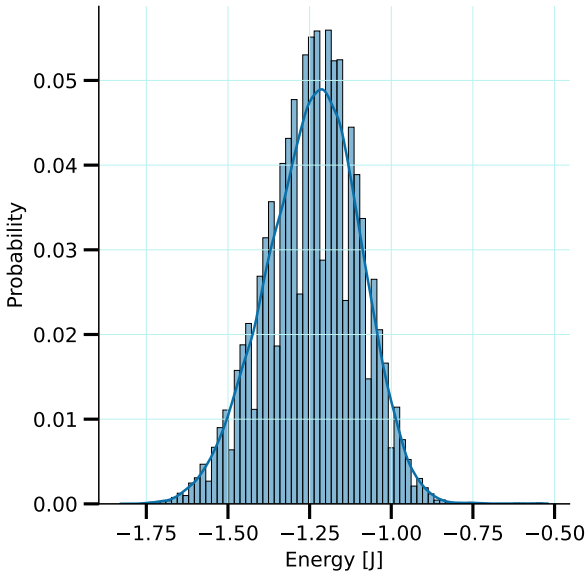

Figure 8: The probability distribution of ϵ at temperature $T = 2.4J/k_B$ generated from 25 independent simulations using the MCMC method with 2000 cycles.

IV. DISCUSSION

Figure 1 shows how the average energy per spin $\langle\epsilon\rangle$ approaches the analytical expected value as the number of Monte Carlo cycles increases. We see that after about $10^{4.5}$ cycles, the computed average starts to converge towards the analytical average. The same holds for the average absolute magnetization per spin, plotted in Figure 2, the specific heat capacity in Figure 3, and the magnetic susceptibility in Figure 4. As the computation time grows for larger number of cycles, we were interested in finding a number of cycles that would produce sufficiently accurate results within a feasible amount of computation time. From the comparison, we conclude that a lower limit of approximately $10^{4.5}$ cycles can provide us with adequate average values.

In Figure 9 and 10 we see the convergence of the energy and magnetization per spin for the model at different temperatures, both ordered and unordered initial states. We see that the ordered initial states start the furthest away from the equilibrium point (convergence point). This is expected, as the equilibrium state is the state with the highest multiplicity, whereas the completely ordered states have the lowest possible multiplicity. We can also see that the ordered initial states have the smallest absolute energy as is expected from the Boltzmann distribution. For the unordered states we see that they are initiated close to equilibrium when the temperature is low. For higher temperatures such

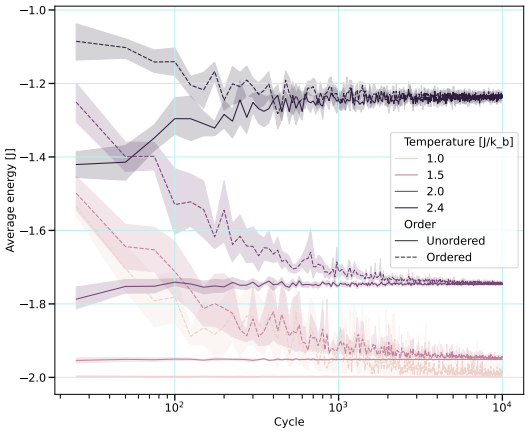

Figure 9: Convergence of $\langle\epsilon\rangle$ of ordered and unordered initial states for different temperatures and lattice size $L = 20$. We have included a 95% confidence interval computed from 25 different samples.

as $T = 2.4$, both the ordered and the unordered states are initialized far away from the equilibrium state. For lower temperatures there are fewer possible configurations for the model. We expect this to hold for greater lattice sizes as well as the energy has to be distributed over a larger number of spins.

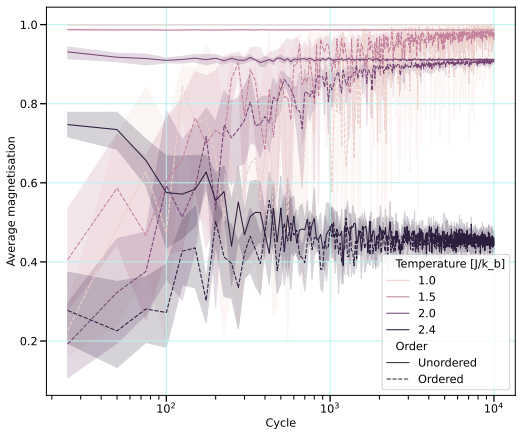

Figure 10: Convergence of $\langle |m| \rangle$ of ordered and unordered initial states for different temperatures and lattice size $L = 20$. We have included a 95% confidence interval computed from 25 different samples.

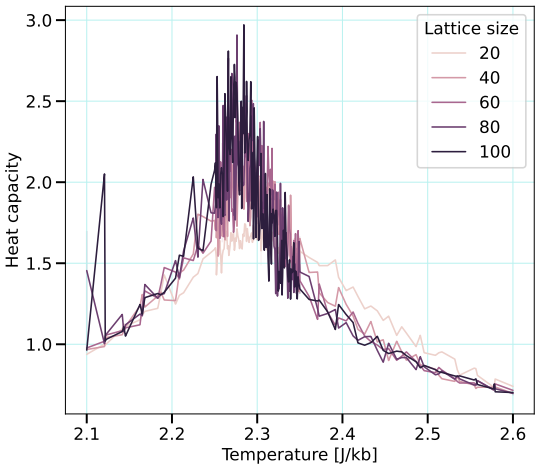

Figure 11: Detailed scan of the specific heat capacity for the different lattices over a range of temperatures.

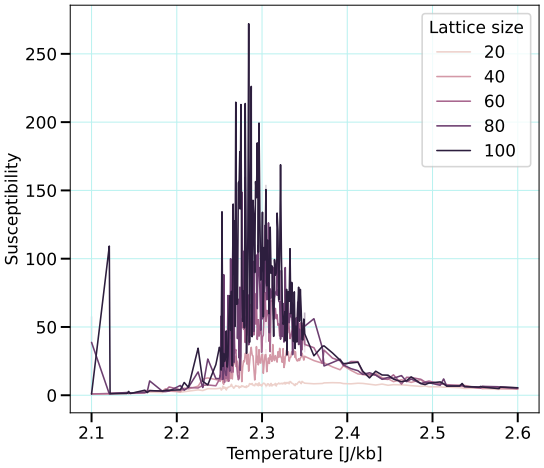

Figure 12: Detailed scan of the susceptibility for different lattices over a range of temperatures.

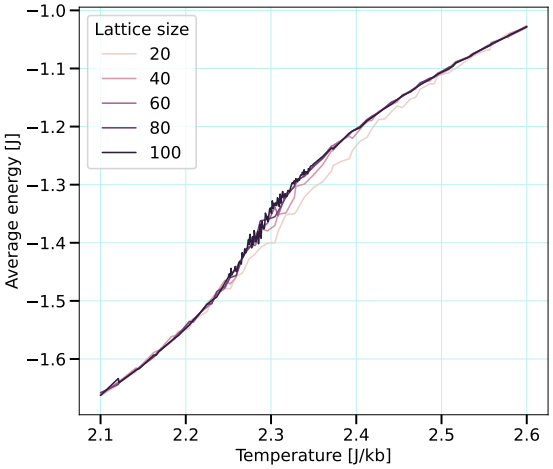

Figure 13: Detailed scan of the average energy per spin for different lattices over a range of temperatures.

From Figures 5, 6, 7 and 8 we observe that higher energies become more probable as the temperature increases. In addition, we see how the variance of the distributions increases when the temperature increases. we notice that there are more available energies at higher temperatures and a small range of probable temperatures for lower temperatures. This is expected as the temperature is a measure of mean kinetic energy and so the mean energy per spin must increase and decrease along with the temperature. At higher temperatures there is more energy to distribute at a similar amount of spins and so the spins' range of possible energies increase, which is represented by the standard deviation of the distributions of the different temperatures. We noted that the distribution at higher temperatures approached a gaussian distribution.

We may also note how the energy probability distribution in the low temperature Figure 5 and Figure 6 have a small extra peak. These peaks in the probability arise closely to the larger peak and are relatively small in comparison. We think this might arise from the initial states of the models, but would require further investigation.

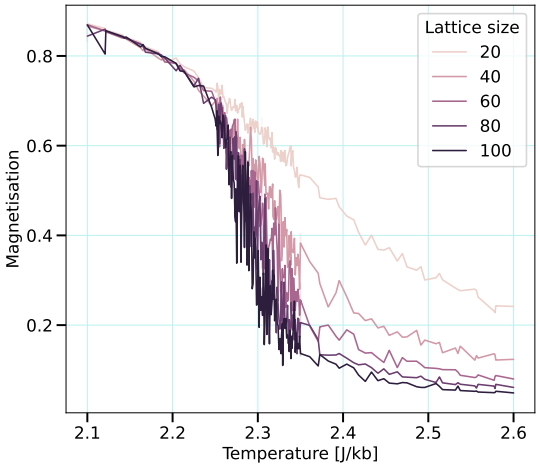

Figure 14: Detailed scan of the average absolute magnetization per spin for different lattices over a range of temperatures.

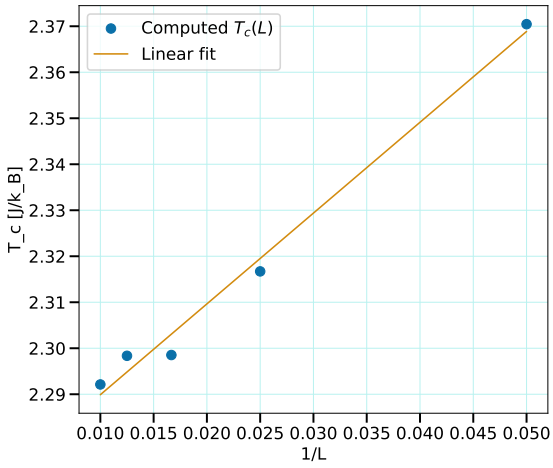

Figure 15: Linear fit of T_C as function of lattice sizes. The fit was performed using first order linear regression. The dots are our approximated values of T_C for our simulated models.

With Figures 9 and 10 we estimated an appropriate burn-in time by looking at the initial convergence. We observed that both ordered and unordered models for each temperature converged at approximately 10^3 cycles. From these Figures we set a burn-in time of 5000 cycles. We were limited by the computational cost of the simulations and could not compute up to the desired amount of $10^{4.5}$ cycles. We rather chose to simulate 25 independent models and compute a mean with a confidence interval. The oscillations around the equilibrium point are great in Figures 9 and 10, which might indicate that we did not simulate for a great enough total amount of Monte Carlo cycles.

In Figure 13, 14, 11 and 12 we get an overview of how the model varies with the temperature. We see that the energy has an increasing value in the whole plot, but we see that the steepest point or a peak in the derivative at $T \approx 2.3$. We observe that $\langle \epsilon \rangle$ increases constantly except at approximately $T = 2.3J/k_B$ where the steepness increases greatly before settling again. This is a clear sign of a phase transition. We know that the change in the specific heat capacity is closely linked to the energy of the model. From the nature of the specific heat capacity we expect C_V to reach a peak at a similar temperature as where the $d\epsilon/dT$ is the steepest. This is precisely what we see in Figure 11. If we look at the individual lattice sizes, we see that in the average energy per spin there is low difference in incline for the $L = 20$ lattice. We then expect the $L = 20$ lattice to have low peak in the specific heat capacity. This we observe i Figure 11, where $L = 20$ has the smallest peak which matches our expectation. Moreover, we see in Figure 11 that $L = 100$ has the highest peak of all the lattice sizes. This means that it should have the highest incline in Figure 13. It is not that clear but still visible that $L = 100$ inclines the most in Figure 13 as expected. The same holds for the relation between the magnetization and the magnetic susceptibility. In Figure 14 we see that lattice $L = 100$ has the steepest incline, and in Figure 12 we see that $L = 100$ yields the highest maximum value. We see that the magnetization for $L = 20$ has the smallest incline in Figure 14, and that the its peak in Figure 12 is relatively low compared to the other lattice sizes. We noticed that all these observations happen in the same temperature region which was a clear indication of the critical temperature to be in said region. We computed an approximated critical temperature using five of the highest values of χ. This was done as we only used a single sample with high temperature resolution. We knew we did not have enough iterations to reach a good approximation (less than $10^4.5$) and so we considered that an approximated critical temperature as an average over the highest peaks of χ would yield more trustworthy results.

From Figure 15 we observed that we had few datapoints on which to perform the regression. Ideally we would have found approximations for critical temperatures for a greater range of lattice sizes. We also expect that a multiple independent simulations would give us a better approximation to each critical temperature. However we were limited by the computational expense of our simulations. Our computed critical temperature as the lattice size L approaches infinity has a relative error of 0.05%, as stated in table II. This is a low relative error, meaning that our results are acceptable and

our models are well suited. Our result only differs from the analytical value by $0.001J/k_B$, which is less than our uncertainty of $0.003J/k_B$.

A. Future work

For future work there are a few points to investigate. The first is that our burn-in time was only estimated based on the convergence of the energy per spin and magnetization per spin of a lattice size of 20. It would be interesting to see how the convergence is for higher lattices sizes, and then know that our chosen burn-in time holds well for the other lattices that we have simulated.

It is also interesting to do the simulations that we have done in a larger scale. The simulations could be done for a higher number of MC cycles for the accuracy of our samples to be higher and therefor give more accuracy in our linear fit for the comparison with Onsager.

Finally, our computations are require a great amount of computational time and we have make use of parallelization method our simulations to make the run-time smaller. To solve these issues we could look into memory optimisation methods and alternative methods for simulating the Ising model.

V. CONCLUSION

In this report we have simulated the two-dimensional Ising model using the Markov chain Monte Carlo method. We performed multiple MCMC cycles for different lattice sizes, and computed macroscopic values of our system based on the microscopic configurations. We computed the mean energy $\langle\epsilon\rangle$, mean absolute magnetization $\langle|m|\rangle$, specific heat capacity C_V and susceptibility χ values numerically for different numbers of Monte Carlo cycles, and compared them with analytical values. We found that they converge to the analytical values after around $10^{4.5}$ cycles. We were limited by our computational power and had to reduce to 10^4 cycles.

We also computed the energy probability distribution for four different temperatures. We found that the energy increases with temperature, meaning that higher energies become more probable as temperature increases. We could also see that the higher energies had a higher variance.

We were interested in looking at the critical temperature where the system went through a phase transition. We computed the critical temperature for different simulations using different lattice sizes, and used these to find an approximation to the critical temperature as the lattice size approached infinity. We found a critical temperature of $T_c(L = \infty) = 2.270 \pm 0.003J/k_B$, which had a relative error of 0.05%. This value differs from the analytical value calculated by Lars Onsager by $0.001J/k_B$, and so we have concluded that our method for finding the critical temperature is reliable.

If we were to repeat these computations in the future, we would like to investigate further the burn-in time we have chosen, and how well it holds for different lattice sizes. We would also have liked to run our simulations on a larger scale.

[1] E. Ising, Zeitschrift fur Physik **31**, 253 (1925).
[2] S. P. Singh, in *Metastable, Spintronics Materials and Mechanics of Deformable Bodies*, edited by S. Sivasankaran, P. K. Nayak, and E. Günay (IntechOpen, Rijeka, 2020) Chap. 8.
[3] J. J. Hopfield, Proceedings of the National Academy of Science **79**, 2554 (1982).
[4] Y.-P. Ma, I. Sudakov, C. Strong, and K. M. Golden, "Ising model for melt ponds on arctic sea ice," (2014).
[5] L. Onsager, Physical Review **65**, 117 (1944).
[6] D. Schroeder, *An Introduction to Thermal Physics* (Oxford University Press, 2021).

Table III: Table of all the possible microstates for a 2×2 grid, together with their energy and magnetization.

Microstate	Energy E $[J]$	Magnetization M	Microstate	Energy E $[J]$	Magnetization M
$+1\ +1$ $+1\ +1$	-8	4	$+1\ +1$ $+1\ -1$	0	2
$+1\ +1$ $-1\ +1$	0	2	$+1\ +1$ $-1\ -1$	0	0
$+1\ -1$ $+1\ +1$	0	2	$+1\ -1$ $+1\ -1$	0	0
$+1\ -1$ $-1\ +1$	8	0	$+1\ -1$ $-1\ -1$	0	-2
$-1\ +1$ $+1\ +1$	0	2	$-1\ +1$ $+1\ -1$	8	0
$-1\ +1$ $-1\ +1$	0	0	$-1\ +1$ $-1\ -1$	0	-2
$-1\ -1$ $+1\ +1$	0	0	$-1\ -1$ $+1\ -1$	0	-2
$-1\ -1$ $-1\ +1$	0	-2	$-1\ -1$ $-1\ -1$	-8	-4

Appendix A: Microstates for the 2×2 grid

For $L = 2$, we have a 2×2 lattice. This gives us 16 different microstates on the form

$$\begin{matrix} s_{11} & s_{12} \\ s_{21} & s_{22} \end{matrix}.$$

This grid represents a periodic lattice, and so when calculating the energy of each neighbouring pair, we take each value and pair it with the value above and to the right. That is, we look at the pairs s_{21} with s_{22} and s_{11}, s_{22} with s_{21} (because the grid repeats) and s_{12}, s_{11} with s_{12} and s_{21}, and s_{12} with s_{22} and s_{11}. We calculate the energy and magnetization of each microstate using equations 6 and 7 respectively. In table III you can see all the possible configurations (microstates) of the 2×2 grid, with their corresponding energy and magnetization. From this table we can count the multiplicity (degeneracy) of each macrostate. The number of $+1$-spins (spin up) together with the energy, magnetization and their multiplicity for this 2×2 grid are listed in table I.

Appendix B: Deriving the partition function and some expectation values for a 2×2 lattice

We derive the partition function for a lattice of dimensions $2\ \times 2$:

$$\begin{aligned} Z &= \sum_{\mathbf{s}} e^{-\beta E(\mathbf{s})} \\ &= 12e^{-\beta \cdot 0} + 2e^{-\beta(-8J)} + 2e^{-\beta \cdot 8J} \\ Z &= 2\left(6 + e^{8\beta J} + e^{-8\beta J}\right). \end{aligned}$$

Using the partition function, we can derive the expectation value of energy per spin ϵ:

$$\begin{aligned}
\langle \epsilon \rangle &= \sum_{\mathbf{s}} \epsilon(\mathbf{s}) p(\mathbf{s}) \\
&= \frac{1}{N} \sum_{\mathbf{s}} E(\mathbf{s}) \, \frac{e^{-\beta E(\mathbf{s})}}{Z} \\
&= \frac{1}{4} \sum_{\mathbf{s}} \frac{e^{-\beta E(\mathbf{s})}}{Z} E(\mathbf{s}) \\
&= \frac{1}{4} \left(\cancel{\frac{12e^0}{Z} \cdot 0} + \frac{2e^{8\beta J}}{Z} \cdot (-8J) + \frac{2e^{-8\beta J}}{Z} \cdot 8J \right) \\
&= \frac{1}{4} \left(\frac{16Je^{-8\beta J}}{Z} - \frac{16Je^{8\beta J}}{Z} \right) \\
\langle \epsilon \rangle &= \frac{4J}{Z} (e^{-8\beta J} - e^{8\beta J}).
\end{aligned}$$

Further, we repeat this for the expectation value of energy per spin squared, ϵ^2:

$$\begin{aligned}
\langle \epsilon^2 \rangle &= \sum_{\mathbf{s}} \epsilon(\mathbf{s})^2 p(\mathbf{s}) \\
&= \frac{1}{N^2} \sum_{\mathbf{s}} \frac{e^{-\beta E(\mathbf{s})}}{Z} E(\mathbf{s})^2 \\
&= \frac{1}{16} \left(\cancel{\frac{12e^0}{Z} \cdot 0} + \frac{2e^{8\beta J}}{Z} (-8J)^2 + \frac{2e^{-8\beta J}}{Z} (8J)^2 \right) \\
&= \frac{1}{8} \left(\frac{64J^2 e^{8\beta J}}{Z} + \frac{64J^2 e^{-8\beta J}}{Z} \right) \\
\langle \epsilon^2 \rangle &= \frac{8J^2}{Z} \left(e^{8\beta J} + e^{-8\beta J} \right).
\end{aligned}$$

These expectation values can be used to calculate the variance of energy σ_E^2:

$$\begin{aligned}
\sigma_E^2 &= \langle E^2\rangle - \langle E\rangle^2 \\
&= N^2\langle \epsilon^2\rangle - \langle \epsilon\rangle^2 \\
&= 16\left[\frac{8J^2}{Z}(e^{8\beta J}+e^{-8\beta J}) - \left(\frac{4J}{Z}(e^{-8\beta J}-e^{8\beta J}\right)^2\right] \\
&= 16\left[\frac{8J^2}{Z}(e^{8\beta J}+e^{-8\beta J}) - \frac{16J^2}{Z^2}(e^{-8\beta J}-e^{8\beta J})^2\right] \\
&= 16\left[\frac{16J^2}{Z^2}\left(\frac{Z}{2}e^{8\beta J}+\frac{Z}{2}e^{-8\beta J} - (e^{-8\beta J}-e^{8\beta J})^2\right)\right] \\
&= \frac{256J^2}{Z^2}\left[\left(6+e^{8\beta J}+e^{-8\beta J}\right)e^{8\beta J} + \left(6+e^{8\beta J}+e^{-8\beta J}\right)e^{-8\beta J} - e^{-16\beta J} + 2 - e^{16\beta J}\right] \\
&= \frac{256J^2}{Z^2}\left[6e^{8\beta J} + \cancel{e^{16\beta J}} + 1 + 6e^{-8\beta J} + 1 + \cancel{e^{-16\beta J}} - \cancel{e^{-16\beta J}} + 2 - \cancel{e^{16\beta J}}\right] \\
&= \frac{256J^2}{Z^2}\left[4 + 6e^{8\beta J} + 6e^{-8\beta J}\right] \\
&= \frac{256J^2}{Z^2}\cdot 6\left[\frac{2}{3} + 6e^{8\beta J} + 6e^{-8\beta J} + 6 - \frac{18}{3}\right] \\
&= \frac{512J^2}{Z^2}\cdot 3\left[Z - \frac{16}{3}\right] \\
\sigma_E^2 &= \frac{512J^2(3Z-16)}{Z^2}.
\end{aligned}$$

Using the variance of energy, we compute the analytical heat capacity C_V:

$$\begin{aligned}
C_V &= \frac{1}{N}\frac{1}{k_BT^2}\sigma_E^2 \\
&= \frac{1}{4k_BT^2}\frac{512J^2(3Z-16)}{Z^2} \\
C_V &= \frac{128}{k_BT^2}\frac{J^2(3Z-16)}{Z^2}.
\end{aligned}$$

Similarly, we obtain the expectation value of the absolute value of magnetization per spin $|m|$:

$$\begin{aligned}
\langle |m|\rangle &= \sum_{\mathbf{s}} |m(\mathbf{s})|p(\mathbf{s}) \\
&= \frac{1}{N}\sum_{\mathbf{s}}\frac{e^{-\beta E(\mathbf{s})}}{Z}|M(\mathbf{s})| \\
&= \frac{1}{4}\left(\cancel{\frac{4e^0}{Z}}\cdot 0 + \cancel{\frac{2e^{-8\beta J}}{Z}}\cdot 0 + \frac{8e^0}{Z}\cdot 2 + \frac{2e^{8\beta J}}{Z}\cdot 4\right) \\
&= \frac{1}{4}\frac{16+8e^{8\beta J}}{Z} \\
\langle |m|\rangle &= \frac{4+2e^{8\beta J}}{Z}.
\end{aligned}$$

We now derive the expectation value of the absolute value of magnetization squared $\left|m^2\right|$:

$$\begin{aligned}
\langle m^2\rangle &= \sum_{\mathbf{s}} m(\mathbf{s})^2 p(\mathbf{s}) \\
&= \frac{1}{N^2}\sum_{\mathbf{s}} \frac{e^{-\beta E(\mathbf{s})}}{Z} M(\mathbf{s})^2 \\
&= \frac{1}{16}\left(\cancel{\frac{4e^0}{Z}\cdot 0^2} + \cancel{\frac{2e^{-8\beta J}}{Z}\cdot 0^2} + \frac{8e^0}{Z}\cdot 2^2 + \frac{2e^{8\beta J}}{Z}\cdot 4^2\right) \\
&= \frac{1}{16}\left(\frac{32}{Z} + \frac{32e^{8\beta J}}{Z}\right) \\
\langle m^2\rangle &= \frac{2}{Z}\left(1+e^{8\beta J}\right).
\end{aligned}$$

Further, the variance of magnetization σ_M^2:

$$\begin{aligned}
\sigma_M^2 &= \langle M^2\rangle - \langle |M|\rangle^2 \\
&= N^2(\langle m^2\rangle - \langle |m|\rangle^2) \\
&= 16\left[\frac{2}{Z}(1+e^{8\beta J}) - \left(\frac{4+2e^{8\beta J}}{Z}\right)^2\right] \\
&= 16\left[\frac{2}{Z^2}Z(1+e^{8\beta J}) - \frac{1}{Z^2}(16+16e^{8\beta J}+4e^{16\beta J})\right] \\
&= 16\left[\frac{4}{Z^2}\frac{Z}{2}(1+e^{8\beta J}) - \frac{4}{Z^2}(4+4e^{8\beta J}+e^{16\beta J})\right] \\
&= \frac{64}{Z^2}\left[(6+e^{8\beta J}+e^{-8\beta J})(1+e^{8\beta J}) - (4+4e^{8\beta J}+e^{16\beta J})\right] \\
&= \frac{64}{Z^2}\left(6+6e^{8\beta J}+e^{8\beta J}+\cancel{e^{16\beta J}}+e^{-8\beta J}+1-4-4e^{8\beta J}-\cancel{e^{16\beta J}}\right) \\
\sigma_M^2 &= \frac{64}{Z^2}(3+3e^{8\beta J}+e^{-8\beta J}).
\end{aligned}$$

Lastly, this variance can be used to compute the magnetic susceptibility χ:

$$\begin{aligned}
\chi &= \frac{1}{N}\frac{1}{k_B T}\sigma_M^2 \\
&= \frac{1}{4k_B T}\frac{64}{Z^2}(3+3e^{8\beta J}+e^{-8\beta J}) \\
\chi &= \frac{16}{Z^2 k_B T}(3+3e^{8\beta J}+e^{-8\beta J}).
\end{aligned}$$

Appendix C: Deriving the simplified acceptance rule

We can derive our simplified acceptance rule for new states in the MCMC method. The general acceptance rule is to check if $r < \min(1, p(\mathbf{s}_{i+1},T)/p(\mathbf{s}_i,T))$. We can therefore start with $p(\mathbf{s}_{i+1},T)/p(\mathbf{s}_i,T)$, and simplify this to our case using equation 8.

$$\begin{aligned}
\frac{p(\mathbf{s}_{i+1},T)}{p(\mathbf{s}_i,T)} &= \frac{\frac{1}{Z}e^{-\beta E(\mathbf{s}_{i+1})}}{\frac{1}{Z}e^{-\beta E(\mathbf{s}_i)}} \\
&= \frac{e^{-\beta E(\mathbf{s}_{i+1})}}{e^{-\beta E(\mathbf{s}_i)}} \\
&= e^{-\beta(E(\mathbf{s}_{i+1})-E(\mathbf{s}_i))} \\
&= e^{-\beta\Delta E}.
\end{aligned}$$

Here we are left with only the Boltzmann factor for the change in energy that the spin flip made, and so our acceptance condition can be written as

$$r < \min(1, e^{-\beta \Delta E}).$$